

## *Retraction*

# **Retracted: Automatic Recognition and Detection System Based on Machine Vision**

### **Journal of Control Science and Engineering**

Received 17 October 2023; Accepted 17 October 2023; Published 18 October 2023

Copyright © 2023 Journal of Control Science and Engineering. This is an open access article distributed under the Creative Commons Attribution License, which permits unrestricted use, distribution, and reproduction in any medium, provided the original work is properly cited.

This article has been retracted by Hindawi following an investigation undertaken by the publisher [1]. This investigation has uncovered evidence of one or more of the following indicators of systematic manipulation of the publication process:

- (1) Discrepancies in scope
- (2) Discrepancies in the description of the research reported
- (3) Discrepancies between the availability of data and the research described
- (4) Inappropriate citations
- (5) Incoherent, meaningless and/or irrelevant content included in the article
- (6) Peer-review manipulation

The presence of these indicators undermines our confidence in the integrity of the article's content and we cannot, therefore, vouch for its reliability. Please note that this notice is intended solely to alert readers that the content of this article is unreliable. We have not investigated whether authors were aware of or involved in the systematic manipulation of the publication process.

Wiley and Hindawi regrets that the usual quality checks did not identify these issues before publication and have since put additional measures in place to safeguard research integrity.

We wish to credit our own Research Integrity and Research Publishing teams and anonymous and named external researchers and research integrity experts for contributing to this investigation.

The corresponding author, as the representative of all authors, has been given the opportunity to register their agreement or disagreement to this retraction. We have kept a record of any response received.

### **References**

- [1] L. Wang and L. Cui, "Automatic Recognition and Detection System Based on Machine Vision," *Journal of Control Science and Engineering*, vol. 2022, Article ID 7318374, 7 pages, 2022.

## Research Article

# Automatic Recognition and Detection System Based on Machine Vision

Lu Wang <sup>1</sup> and Lihong Cui <sup>2</sup>

<sup>1</sup>*School of Information and Communication Engineering, Liaoning Equipment Manufacturing Vocational and Technical College, Shenyang, Liaoning 110161, China*

<sup>2</sup>*Chaoyang Open University, Chaoyang, Liaoning 122000, China*

Correspondence should be addressed to Lihong Cui; 2018050200005@jlxj.nju.edu.cn

Received 20 May 2022; Revised 16 June 2022; Accepted 22 June 2022; Published 6 July 2022

Academic Editor: Jackrit Suthakorn

Copyright © 2022 Lu Wang and Lihong Cui. This is an open access article distributed under the Creative Commons Attribution License, which permits unrestricted use, distribution, and reproduction in any medium, provided the original work is properly cited.

In order to realize the automation of part identification and detection and the intellectualization of part production, this paper proposes a method of automatic identification and detection of parts based on machine vision (overall method). This paper combines machine vision with motion control theory and uses pulse coupled neural network (PCNN) edge detection and recognition algorithms to preliminarily design a set of machine vision automatic recognition and detection systems and carry out detection and recognition experiments on small parts such as relay covers. The experimental results show that the whole process of part size detection and recognition, including part feeding, image acquisition, size recognition, part screening, and reset of the experimental platform, can be completed within 5 s and can carry out high-precision dynamic recognition and detection when the part moves at a speed of 1 m/s. Through the correction and compensation of dynamic error, the detection accuracy of small rectangular parts with a length of 28.87 mm and a width of 12.36 mm can reach 0.04 mm. The visual inspection and recognition automation system improves the automation degree of parts inspection, improves the dimensional accuracy, optimizes the robustness of the system, and finally realizes the real-time screening and classification of parts and the efficient production of parts.

## 1. Introduction

Industrial automatic detection technology is a comprehensive technology based on the principles of physics, electronics, automatic control, electronic computers, and measurement technology. Its research purpose is to automatically check and measure various process parameters in an industrial automation system [1]. There are many kinds of mechanical parts with a large output, and their quality directly affects the performance of assembled products. Part quality inspection is a necessary link in the modern manufacturing industry. Improving inspection reliability and efficiency and reducing inspection time are important ways to improve production efficiency [2]. At present, most manufacturing enterprises still use manual detection, which is greatly affected by the physiology and subjectivity of workers, so it is difficult to ensure the reliability of detection,

and it takes a long time and has low efficiency [3]. Machine vision is widely used in information recognition and feature detection of industrial parts because of its stable system, efficient process, and accurate results. In view of the urgent need of many small- and medium-sized enterprises to “replace people with machines” to improve the automation and intelligence of the detection process, a set of continuous automatic detection systems for multivariety small- and medium-sized parts based on machine vision has been developed for engineering applications. The system improves the detection efficiency and records the status of each part, which plays a guiding role in production and reduces unnecessary waste. The design of an automatic recognition and detection system based on machine vision is shown in Figure 1.

Yang and others used a charge coupled device (CCD) camera and image processing method to measure the

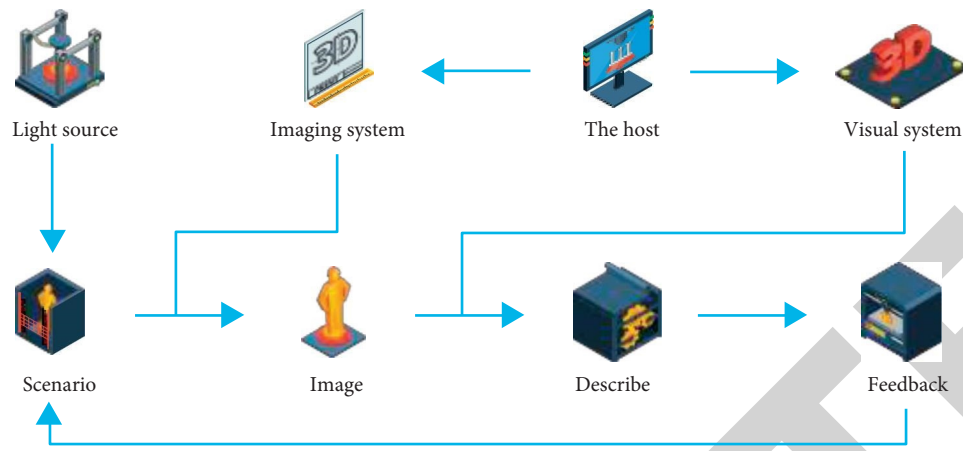


FIGURE 1: Design of automatic recognition and detection system based on machine vision.

bearing diameter. For the bearing with an outer diameter of 22.760 mm, the mean value of 16 measurements was 22.769 mm, the standard deviation was 0.015 mm, and the relative error was 0.066% [4]. Zalyubovs'Kyj and others used a high-resolution CCD camera and magnification imaging method to measure the geometric parameters and roundness error of a toothed chain plate. For the pitch with a nominal size of 9.525 mm, the measurement error is 7  $\mu\text{m}$ , the relative error is 0.0735%, and for the round pin hole with a nominal diameter of 3.76 mm, the measurement roundness error is 8.4  $\mu\text{m}$  [5]. Djetel Gothe and others used the linear array industrial camera and contour vectorization method to study the size detection system of sheet parts based on machine vision, and applied the system to detect the two-dimensional size of the elastic arm sheet of a computer hard disk. For the qualified size with the design tolerance of  $\pm 0.005$  mm and the size range of 3.81 mm–45.72 mm, the measurement results are consistent with reality, and the average detection time of each part is 1 s. This kind of visual measurement method based on single image processing realizes the organic combination of light, machine, electricity and computer technology. The measurement of size and shape errors can be carried out simultaneously in one system, and the measurement results are convenient for computer analysis and processing [6]. Pham and others integrated the machine vision system with the coordinate measuring machine, made full use of the characteristics of easy processing of visual images and easy combination with automation technology, realized the automatic alignment of detection benchmark, and greatly improved the measurement efficiency while obtaining high-precision measurement results [7]. Tourani and others used the dual coordinate structure composed of an area array CCD device and a high-precision measurement grating to form a high-precision geometric measurement system based on machine vision. Using the detection method of contour tracking, the actual position of the part contour is determined by the dual coordinate system, so as to realize the precise measurement of the part geometric halo and achieve micron level measurement accuracy [8]. Hou and others proposed an automatic splicing method using subpixel micro displacement

combined with phase correlation according to the high accuracy detection requirements of millimeter sized micro parts. This method inherits the strong anti-interference ability of the phase correlation method, successfully realizes the subpixel splicing of the tested object, and meets the high-precision measurement requirements of micro parts [9]. Gao and others used CCD cameras to carry out dynamic detection of parts, specifically analyzed the influencing factors of static and dynamic measurement accuracy, and corrected and compensated the measurement results to achieve an accurate and stable measurement, but lacked specific verification instructions for the timeliness of detection [10].

In view of the above problems, this paper designs a set of parts visual inspection and recognition automation system, and through the combination of LabVIEW visual processing software and MATLAB data calculation software, integrates the image acquisition and processing algorithm with the edge detection algorithm of the pulse coupled neural network PCNN (pulse coupled neural network), and verifies the performance of the system in all aspects.

## 2. Research Methods

*2.1. Basic Working Principle and Algorithm Improvement of PCNN.* PCNN is composed of several basic neuron models. It is a bionic technology for the visual characteristics of advanced mammals. Each neuron is a single-layer model neural network, which can realize the natural embodiment of network characteristics without a training process [11–13]. It also has the characteristics of time-space summation, dynamic pulse emission, and vibration and fluctuation caused by synchronous pulse emission. In image processing, PCNN can be widely used in digital image segmentation, edge detection, retrieval, enhancement, fusion, pattern recognition, target classification, denoising, and other processing. It can also be combined with other signal processing technologies such as wavelet theory, mathematical morphology, and fuzzy processing, and is more widely used in image and other related processing [14, 15]. A PCNN is a feedback network composed of several interconnected neurons. In medical image fusion, the

simplified PCNN model [16] adopted in this paper is shown in Figure 2. When processing two-dimensional images, the external input of the traditional PCNN algorithm is usually the gray value of each pixel. However, a single pixel can often not reflect the characteristics of the image. Therefore, this paper uses the spatial frequency SF reflecting the characteristics of the spatial neighborhood as the external input of PCNN; SF is obtained according to the following formula [17]:

$$S_{ij}^k = \sum_{i \in M, j \in N} (I_{ij}^k - I_{i-1,j}^k)^2 + (I_{ij}^k - I_{i,j-1}^k)^2. \quad (1)$$

When using PCNN for image fusion, the external input of the neuron is the gray value of the pixel of the source image, which corresponds to the pixel one by one, and the position of the neuron also corresponds to the meaning of the pixel. The mathematical model of PCNN simplified model is the following formula [18]:

$$\begin{cases} F_{ij}^k(n) = S_{ij}^k, \\ L_{ij}^k(n) = \exp(-\alpha_L)L_{ij}^k(n-1) + V_L \sum_{mn} W_{ij,mn} Y_{ij}^k(n-1), \\ U_{ij}^k(n) = F_{ij}^k(n) \times (1 + \beta L_{ij}^k(n)) \\ \theta_{ij}^k(n) = \exp(-\alpha_\theta)\theta_{ij}^k(n-1) + V_\theta Y_{ij}^k(n-1), \\ Y_{ij}^k(n) = \begin{cases} 1, & \text{if } U_{ij}^k(n) > \theta_{ij}^k(n), \\ 0, & \text{if } U_{ij}^k(n) \leq \theta_{ij}^k(n), \end{cases} \end{cases} \quad (2)$$

where  $k$  is the number of decomposition layers of the image; subscript  $(i, j)$  represents the  $(i, j)$ -th element in the decomposition coefficient, and  $S_{ij}^k$  is the external input;  $U_{ij}^k$  and  $Y_{ij}^k$  are the internal state signal and external output of neurons during H-layer decomposition;  $F_{ij}^k$  and  $L_{ij}^k$  are the feed input and link input during layer decomposition;  $\beta$  is the link strength;  $W_{ij,mn}$  is synaptic connection weight;  $\alpha_L$  and  $\alpha_\theta$  are attenuation constants;  $\theta_{ij}^k$  is the dynamic threshold value of  $k$ -layer decomposition;  $V_L$  and  $V_\theta$  are the amplitude gain.

The signal transmission process of neurons can be approximated as the change process of leakage integrator voltage, and it is a linear invariant system. PCNN is a feedback network formed by the interconnection of multiple neurons in which each single neuron is mainly composed of three parts: the receiving domain, the coupling domain (multiplication modulation part), and the pulse generator. The receiving domain mainly receives the output  $Y_{jk}$  from other neurons and the external input (the pixel value  $I_{jk}$  of the gray image). When the input signal reaches the receiving domain, it is divided into two channels to transmit to the modulation part, namely, the connecting input channel  $L_{jk}$  and the feedback input channel  $F_{jk}$ . Then, after multiplying and modulating the signals from the two channels, the internal active item  $U_{jk}$  is obtained (where  $M$  and  $W$  are the weight matrix of the connecting input domain and the feedback input domain respectively,  $\alpha_L$  and  $\alpha_F$  are the time attenuation constants of the connecting input domain and

the feedback input domain respectively;  $\beta$  is the internal active item connecting system). Comparing with the internal activity item  $U_{jk}$  with the dynamic threshold  $\theta_{jk}$ , when it is greater than  $\theta_{jk}$ , the pulse will be released, and the output pulse value  $Y_{jk}$  will participate in the feedback adjustment again. The dynamic threshold  $\theta_{jk}$  will be feedback adjusted through the time attenuation constant  $\alpha_\theta$  and the amplification coefficient  $V_\theta$  to enter the next signal transmission.

In actual image processing, the pulse coupled neural network corresponds to the pixels in the image one by one; that is, how many pixels an image has, then how many neurons the network has. The higher the image pixel, the more neurons. When used for edge detection, the performance of the algorithm changes with the number of iterations, and the detection effect also changes. Each iteration corresponds to a binary image output, which reflects the details of the target and background contour, but the output result of each iteration is not ideal. According to the principle of maximum information entropy, as the number of iterations increases, when the image information entropy reaches its maximum value, it indicates that the image contains the most original image information. Therefore, the maximum information entropy is often used to determine the criterion of the best number of iterations. Before the experiment, it is impossible to determine which output result will be better, which is also one of the defects of PCNN; that is, the detection results cannot be measured by an objective evaluation criterion.

In view of the shortcomings of the traditional PCNN edge detection algorithm, this paper compiles the PCNN algorithm program combined with the detected object and appropriately adjusts the maximum information entropy of the image by setting the capture parameter and suppression parameter. This improves the traditional PCNN algorithm, reduces unnecessary iterations, speeds up the convergence of the algorithm, detects the edge of the target object in real time, and obtains the edge information of the target. In this paper, the improved PCNN algorithm and the traditional edge detection operators (Sobel operator, Roberts operator, Prewitt operator, LOG operator, and Canny operator) are used to detect the edge of the lena.png image, respectively. Among the traditional edge detection operators, the Canny operator extracts the most complete edges with good continuity, but there are many false edges in the extraction results. The edge extracted by improved PCNN is very complete, and the edge of the target can be extracted accurately in the area with a complex background.

**2.2. Design of Visual Inspection and Recognition Automation System.** This paper combines LabVIEW software and MATLAB software to design a part identification and detection system based on PCNN. The system consists of a vision system and a control mechanism. The vision system identifies and detects the incoming parts, obtains the size information, converts it into a control signal, and transmits the control signal to the control card for corresponding action control; The control mechanism is composed of an XYZ three-degree of freedom slide. Firstly, the workpiece is

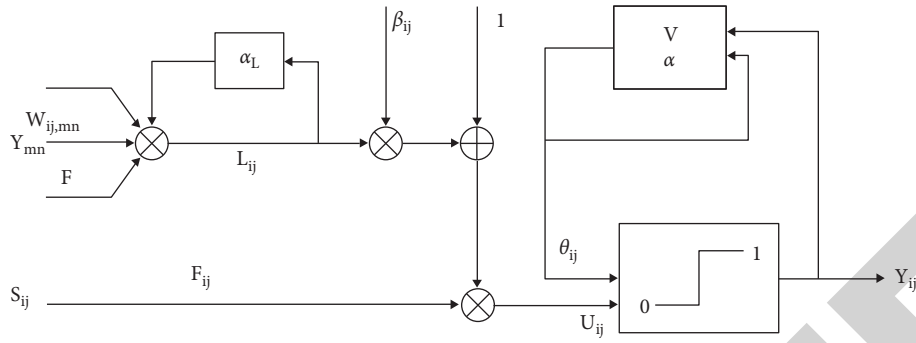


FIGURE 2: Schematic diagram of simplified PCNN model.

transported to the camera and the focal length is adjusted to put the part in the best measurement position. At this time, the vision system collects the image of the part, accurately identifies the edge of the part through the PCNN algorithm, then measures and identifies the size of the edge through the vision assistant module, generates the control signal according to the recognition result, and transmits the control signal to the motion control card to screen the control parts of the mechanism. Finally, the three degree of freedom slide table automatically resets and returns to the original working state [19].

**2.2.1. Establishment of Experimental Platform.** The hardware of the test-bed is mainly composed of the upper computer (industrial control computer), the lower computer (Leisai four-axis motion control card and image acquisition card), servo motor, driver, CCM three-axis slide, shadowless light source, and DC power supply. Among them, the upper computer is used to send motor control instructions, image acquisition and processing instructions, data display, and human-computer interaction. The four-axis motion control card of the lower computer is used to receive the control commands from the upper computer, generate a pulse control signal, and transmit the signal to the servo motor driver through the digital I/O port. The driver completes the control of speed and direction, amplifies the signal and drives the motor to work. As the actuator, the motor makes corresponding actions after receiving the control signal from the driver, so that the CCM three-axis slide mechanism can move up and down, left and right, front and back in three degrees of freedom and six directions. The visual acquisition card is used to receive the signal from the upper computer, collect the image of the part, and then send the image information of the part back to the upper computer through the digital I/O port for operation and processing [20].

**2.2.2. Software Development.** In the professional development version of LabVIEW2011, this paper uses the MATLAB script node to call the Matlab program and completes the automatic identification, detection, and control of parts by combining it with LabVIEW [21]. The control system is shown in Figure 3.

After the program starts to run, the control card first sends a control signal to move the slide table down in the Z

direction and then send the parts. The camera is started through the vision acquisition module of LabVIEW to collect the part image. The collected digital image is converted into an array as the input value of the MATLAB scripts function node, and then MATLAB is called to run the PCNN edge detection program in the node. After the edge is successfully obtained, it is converted into a digital image as the input and enters the vision assistant module of LabVIEW to measure the length and width of the part. Finally, compare the measured value with the standard value to judge the quality of the parts, and give an excitation to the motion control card to realize the movement of the three degree of freedom slide table in the Y direction, completing the screening of parts, automatically resetting after completion, and stopping and waiting for the next identification measurement.

### 3. Result Analysis

The key to the automatic system of part visual recognition and detection is the accuracy of part size measurement, the robustness of the algorithm, and the stability of the system. Firstly, this paper collects the images of parts under the same lighting conditions and different backgrounds. The traditional edge detection operator and the improved PCNN algorithm are used to identify and detect the edges of parts. The comparison of edge extraction results under the same illumination and different backgrounds shows that the edge extracted by the improved PCNN algorithm in the simple background not only ensures the edge integrity but also outperforms the traditional algorithm in the effectiveness of image detail information and is robust. In a certain complex background, the improved PCNN algorithm can also ensure the integrity of the edge, and the edge detection accuracy is relatively high. Therefore, the improved PCNN algorithm can be used for the research of target detection and recognition in complex backgrounds.

Secondly, the standard parts (28.87 mm long and 12.36 mm wide) with the same appropriate illumination intensity and arbitrary position and direction are repeatedly measured with the basic algorithm of LabVIEW and the improved algorithm of PCNN. The results are shown in Figures 4(a) and 4(b).

When the measuring position changes constantly, the measured length value and width value also change

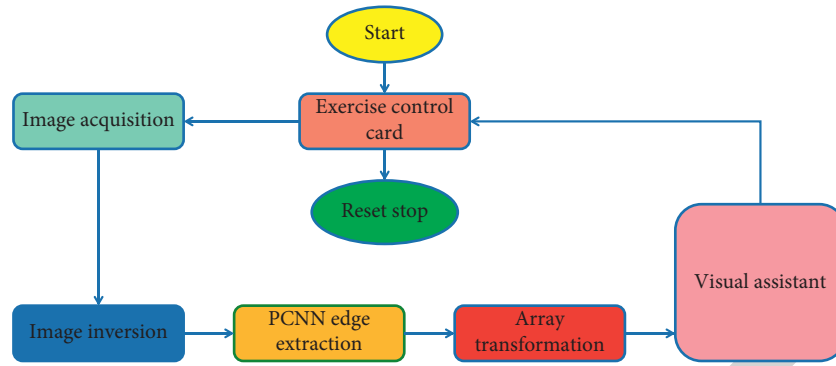


FIGURE 3: Flow chart of control system.

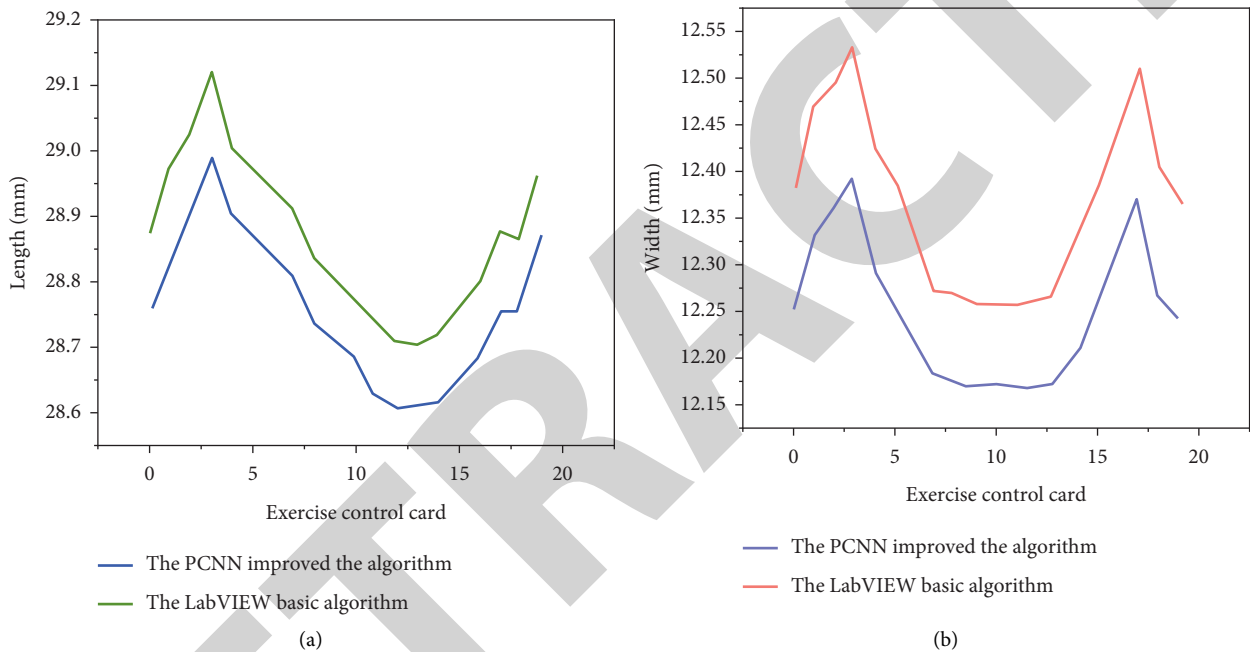


FIGURE 4: Test results of any part in the same position and direction under the same light. (a) Part length measurement results. (b) Part width measurement results.

constantly. When the measured value of the PCNN improved algorithm changes in position, the average deviation from the standard value is very small, floating around the standard value, and the variation fluctuation range is small. Compared with the measured value of the LabVIEW basic algorithm, its stability and accuracy are higher, indicating that the improved PCNN algorithm can improve the stability and robustness of the measurement system and make the measured value more accurate.

Finally, in the process of low-speed movement (1 m/s), the parts are detected at fixed points, and the detection accuracy is  $\pm 0.04$  mm. The automatic identification test is conducted for parts. The length range of qualified parts is set to [28.83 mm, 28.91 mm] and the width range is set to [12.32 mm, 12.40 mm]. 20 parts produced in a batch are tested respectively. The results are shown in Table 1. It can be seen from Table 1 that when the system accuracy is 0.04 mm, it can accurately identify and judge the attributes of parts and complete the whole process of automatic detection and

screening within 5 s. The measurement result on the left side is 28.84 mm in length and 12.34 mm in width. The length and width are qualified, and the display of parts is qualified. The measurement result on the right side is 28.92 mm in length and 12.40 mm in width. The length is unqualified, the width is qualified, and the part displayed is unqualified.

It can be seen that the detection system has strong stability, high precision, and good real-time performance. When the part attributes are detected and identified, the three-axis sliding table makes the corresponding screening action, which improves the automation of the system. The experimental results show that the part visual inspection and recognition automation system overcomes the defects of other inspection systems, such as low detection accuracy, insufficient automation performance, poor reliability, and imperfect detection systems. Complete the whole work of part size detection and identification within 5 s, including part feeding, image acquisition, size identification, part screening, and reset of the test bench. It can carry out high-

TABLE 1: Actual measurement of 20 parts.

Parts	Real attribute	Length/mm	Width/mm	Time/s	Test attribute
1	Qualified	28.83	12.35	5.0	Qualified
2	Qualified	28.85	12.33	4.9	Qualified
3	Qualified	28.91	12.32	4.8	Qualified
4	Unqualified	28.95	12.35	3.5	Unqualified
5	Qualified	28.84	12.34	4.8	Qualified
6	Qualified	28.88	12.34	4.7	4.9 Qualified
7	Qualified	28.89	12.40	4.9	Qualified
8	Qualified	28.84	12.35	5.0	Qualified
9	Unqualified	28.92	12.40	3.9	Unqualified
10	Qualified	28.87	12.37	4.3	Qualified
11	Qualified	28.90	12.35	4.8	Qualified
12	Qualified	28.87	12.38	4.0	Qualified
13	Qualified	28.90	12.39	3.5	Qualified
14	Qualified	28.84	12.33	4.6	Qualified
15	Qualified	28.87	12.36	5.0	Qualified
16	Unqualified	28.88	12.25	3.8	Unqualified
17	Qualified	28.83	12.32	4.8	Qualified
18	Qualified	28.86	12.40	3.8	Qualified
19	Qualified	28.91	12.40	4.8	Qualified
20	Qualified	28.86	12.34	4.9	Qualified

precision dynamic identification and detection when the part moves at a speed of 1 m/s. Through the correction and compensation of dynamic error, the detection accuracy of small rectangular parts with a length of 28.87 mm and a width of 12.36 mm can reach 0.04 mm.

#### 4. Conclusion

Aiming at the shortcomings of traditional detection systems, an automatic detection, identification, and control system is designed in this paper. Using the improved PCNN edge extraction algorithm and combining LabVIEW software with MATLAB software, a set of vision based detection and recognition automation systems is constructed, and the experiment is completed on the built hardware platform. The experiment realizes the identification and measurement of small parts with high efficiency and high precision. The follow-up work of this paper will explore the application of PCNN in complex backgrounds to realize the recognition, segmentation, and tracking of targets in complex backgrounds.

#### Data Availability

The data used to support the findings of this study are available from the corresponding author upon request.

#### Conflicts of Interest

The authors declare that there are no conflicts of interest.

#### Acknowledgments

The study was supported by “Scientific research funding project of Liaoning Provincial Department of Education, China (Grant no. SYZB202003).”

#### References

- [1] W. Wang, J. Taylor, and R. J. Rees, “Recent advancement of deep learning applications to machine condition monitoring part 1: a critical review,” *Acoustics Australia*, vol. 49, no. 2, pp. 207–219, 2021.
- [2] A. Vandone, S. Baraldo, D. Anastassiou, A. Marchetti, and A. Valente, “3d vision system integration on additive manufacturing machine for in-line part inspection,” *Procedia CIRP*, vol. 95, no. 2, pp. 72–77, 2020.
- [3] S. Bickel, C. Sauer, B. Schleich, and S. Wartzack, “Comparing cad part models for geometrical similarity: a concept using machine learning algorithms—sciencedirect,” *Procedia CIRP*, vol. 96, pp. 133–138, 2021.
- [4] J. Yang and A. Palazzolo, “Tilt pad bearing distributed pad inlet temperature with machine learning—part i: static and dynamic characteristics,” *Journal of Tribology*, vol. 144, no. 6, pp. 1–45, 2021.
- [5] M. G. Zalyubovs’Kyi, I. V. Panasyuk, S. O. Koshel, and G. V. Koshel, “Synthesis and analysis of redundant-free seven-link spatial mechanisms of part processing machine,” *International Applied Mechanics*, vol. 57, no. 4, pp. 466–476, 2021.
- [6] S. Djetel-Gothe, S. Bégot, F. Lanzetta, and E. Gavignet, “Design, manufacturing and testing of a beta stirling machine for refrigeration applications,” *International Journal of Refrigeration*, vol. 115, pp. 96–106, 2020.
- [7] T. A. Pham, “Effective deep neural networks for license plate detection and recognition,” *The Visual Computer*, vol. 226, pp. 1–15, 2022.
- [8] A. Tourani, A. Shahbarami, S. Soroori, S. Khazaei, and C. Y. Suen, “A robust deep learning approach for automatic iranian vehicle license plate detection and recognition for surveillance systems,” *IEEE Access*, vol. 8, pp. 201317–201330, 2020.
- [9] X. Hou, W. Ao, Q. Song, J. Lai, H. Wang, and F. Xu, “Fusar-ship: building a high-resolution sar-ais matchup dataset of gaofen-3 for ship detection and recognition,” *Science China Information Sciences*, vol. 63, 2020.
- [10] C. Gao, “Design of tourism package with paper and the detection and recognition of surface defects—taking the paper package of red wine as an example,” *Journal of Intelligent Systems*, vol. 30, no. 1, pp. 720–727, 2021.
- [11] D. Li, Q. Song, T. Li et al., “An lc-ms/ms method for protein detection based on a mass barcode and dual-target recognition strategy,” *RSC Advances*, vol. 10, no. 27, pp. 16094–16100, 2020.
- [12] I. A. Znamenskaya, I. A. Doroshchenko, N. N. Sysoev, and D. I. Tatarenkova, “Results of quantitative analysis of high-speed shadowgraphy of shock tube flows using machine vision and machine learning,” *Doklady Physics*, vol. 66, no. 4, pp. 93–96, 2022.
- [13] M. H. M. Ali and M. R. Atia, “A lead through approach for programming a welding arm robot using machine vision,” *Robotica*, vol. 40, no. 3, pp. 464–474, 2021.
- [14] J. Wang, L. P. Tchapmi, A. P. Ravikumar et al., “Machine vision for natural gas methane emissions detection using an infrared camera,” *Applied Energy*, vol. 257, Article ID 113998, 2020.
- [15] M. Talaat, I. Arafa, and H. Metwally, “Advanced automation system for charging electric vehicles based on machine vision and finite element method,” *IET Electric Power Applications*, vol. 14, no. 13, pp. 2616–2623, 2020.
- [16] C. Zhao, H. Ding, G. Cao, and Y. Zhang, “A new method for detecting compensation hole parameters of automobile brake

- master cylinder based on machine vision,” *Journal of Advanced Transportation*, vol. 2021, Article ID 8864679, 14 pages, 2021.
- [17] Q. Liu, W. Zhang, M. W. Bhatt, and A. Kumar, “Seismic nonlinear vibration control algorithm for high-rise buildings,” *Nonlinear Engineering*, vol. 10, no. 1, pp. 574–582, 2021.
- [18] R. Huang, “Framework for a smart adult education environment,” *World Transactions on Engineering and Technology Education*, vol. 13, no. 4, pp. 637–641, 2015.
- [19] X. Liu, C. Ma, and C. Yang, “Power station flue gas desulfurization system based on automatic online monitoring platform,” *Journal of Digital Information Management*, vol. 13, no. 6, pp. 480–488, 2015.
- [20] J. Jayakumar, B. Nagaraj, S. Chacko, and P. Ajay, “Conceptual implementation of artificial intelligent based E-mobility controller in smart city environment,” *Wireless Communications and Mobile Computing*, vol. 2021, Article ID 5325116, 8 pages, 2021.
- [21] G. Dhiman, V. Vinoth Kumar, A. Kaur, and A. Sharma, “Don: deep learning and optimization-based framework for detection of novel coronavirus disease using x-ray images,” *Interdisciplinary Sciences: Computational Life Sciences*, vol. 13, no. 2, pp. 260–272, 2021.